Terahertz Quantum Cascade Lasers Operating in Magnetic Fields

G. Fasching[1], R. Zobl[1], V. Tamošiunas[1], J. Ulrich[1], G. Strasser[1], K Unterrainer[1], R. Colombelli[2], C. Gmachl[2], L.N. Pfeiffer[2], K.W. West[2], and F. Capasso[3]

[1]Institute of Photonics and Center for Micro- and Nanostructures, Vienna University of Technology, A-1040 Vienna, Austria

[2]Bell Laboratories, Lucent Technologies, 600 Mountain Avenue, Murray Hill, NJ 07974

[3]Harvard University, Division of Engineering and Applied Sciences, Cambridge, MA 02138

We have measured the emission intensity and spectra of Terahertz Quantum Cascade Lasers in an external magnetic field applied normal to the epilayers. We have observed a reduction of the threshold current, an enhancement of laser emission intensity and shifts of the emission line. A wider operating range was predicted for the selected waveguide design according to our finite-difference time-domain simulation results. The intensity enhancement and the threshold current reduction are attributed to the suppression of nonradiative Auger-intersubband transitions by Landau-quantization of the in-plane electron motion, to the modulation of the injection rate via resonant inter-Landau-level transfer, and to the modulation of waveguide properties.

Introduction

The first Quantum Cascade-Laser (QCL) in the Terahertz range was recently demonstrated by Köhler et al [1] proving that QCL concept can be successfully implemented also in far-infrared region. The continuous wave operation of the THz QCL was also reported [2]. However, the further improvement of THz QCLs and lasing at even longer wavelengths is a challenge for different reasons related to the intersubband population dynamics and the waveguide properties. Electron-electron scattering and interface roughness are the main scattering mechanisms at low temperatures in this range of intersubband energies. They lead to fast carrier relaxation, counteracting population inversion. An external magnetic field applied normal to epilayers should lead to an additional quantization of the in-plane electron motion [3] and to the modification of the scattering. The recently observed enhancement of the luminescence intensity of GaAs/AlGaAs [4] and InGaAs/InAlAs [5] Terahertz quantum cascade structures confirms such effect.

Experimental

The system used in the emission experiments consists of a FTIR spectrometer (NICOLET Magna IR 850) equipped with a Si beamsplitter and a 4.2 K Si bolometer. For the magnetic field measurements, the THz QCL is mounted in a magnet cryostat with two superconducting magnets. In this cryostat, detection is possible by a magnetic field tunable InSb cyclotron resonance detector, by a broadband Ga doped Ge detector, or by the external FTIR (Fig. 1).

The magnetic field at the location of the sample (oriented perpendicular to the epitaxial layers) can be adjusted independently from 0 T to 6.7 T by a second magnet. A closed light pipe guides the radiation from the sample to the detector. This narrow band InSb detector [4] is tuned by the magnetic field of the second (detector) superconducting magnet. The whole spectrometer is immersed in liquid He, so that room temperature background radiation cannot distort the measurements.

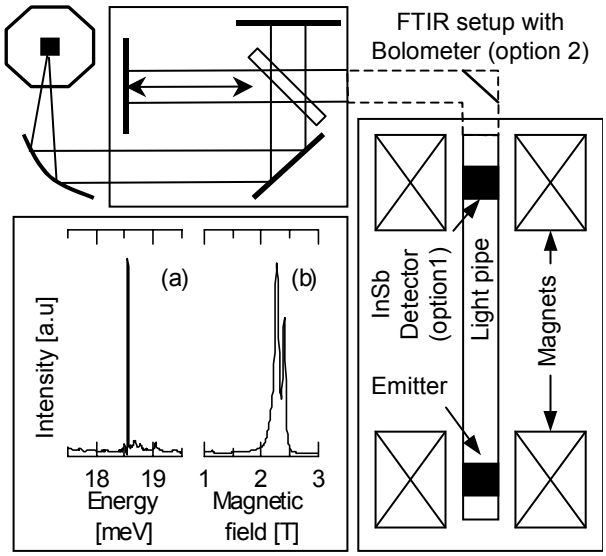

Fig. 1: Set-up for high resolution spectral measurements: cryostat with superconducting magnets, high resolution (0.0155 meV) Fourier spectrometer and Si bolometer. (a) High-resolution spectrum of the laser without applied magnetic field at the emitter sample. (b) Response of the InSb detector versus applied detector magnetic field when illuminated by the THz laser (one line corresponds to the free electron cyclotron resonance, the other one to the impurity bound resonance).

Measurements

A 4.5 THz Quantum Cascade Laser, based on the active structure design proposed in [1] was used for the measurements in a magnetic field. 100 periods of the active structure were sandwiched between two n^+-doped contact layers (the bottom layer was d = 500 nm thick with $n = 4x10^{18}$ cm^{-3} doping, the top layer was d = 100 nm thick with $n = 7x10^{18}$ cm^{-3} doping) grown on a semi insulating GaAs substrate using molecular beam epitaxy (MBE).

A 100 µm wide device was selected for the intensity measurements in magnetic field due to its broadest lasing range. The broadband Ge detector was used to obtain the laser intensity as a function of different sample magnetic fields which is presented in Fig. 2. The laser emission intensity increases substantially for certain values of the magnetic field when compared to B = 0 T. For increasing magnetic fields we observe oscillations with a larger period. The application of a magnetic field increases the laser intensity by a factor of more than five at B = 4.2 T (see Fig. 2). This effect is understood as a consequence of the discretization of the energy spectrum. In the parabolic dispersion relation in the absence of a magnetic field the energy conservation requirement for intersubband Auger-scattering processes is fulfilled for a continuum of energy changes ΔE (meaning one electron suffers an energy change of $+\Delta E$, the other one a change of $-\Delta E$). However, for a non-vanishing magnetic field the only allowed energy changes ΔE are multiples of the cyclotron resonance energy $\hbar\omega_c$. Since the Auger-scattering rate

scales inversely with the associated change in energy and momentum, it is more and more suppressed with increasing Landau-level splitting. The laser intensity is proportional to the inversion which is directly proportional to the injection rate and inversely proportional to the non-radiative relaxation rate.

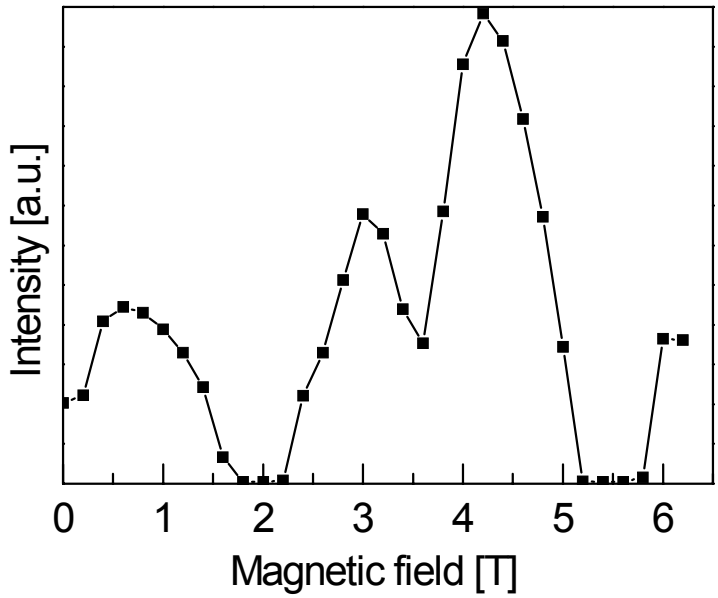

Fig. 2: Maximal laser emission intensity versus magnetic field. Laser emission intensity was recorded for every given magnetic field flux density value by adjusting pulse generator settings to obtain the maximum intensity. Clear emission intensity maxima are observed for N = 2.5 (4.2 T) and N = 3.5 (3 T).

We first assume that the injection rate is not influenced by the magnetic field. We would expect an oscillatory increase of the laser emission with minima where the magneto-intersubband resonance condition is met:

$$E_2 - E_1 = \frac{\hbar e B_N}{m^*} N$$

Here $E_2 - E_1$ is the energy difference between the lowest Landau-levels of the upper and lower laser transition, $\hbar$ - the Planck constant, e - the elementary charge, B_N - magnetic flux density , m^* - effective mass, N – an integer. Resonant tunneling between Landau levels opens up an additional non-radiative relaxation channel via the Landau ladder ($|1,N\rangle$, $|1,N\text{-}1\rangle$, ...$|1,0\rangle$) and by reducing the population inversion leads to the decrease of the laser emission intensity. It should be pointed out that a theoretical model proposed by Raikh and Shahbazyan [9] well describes a momentum transfer caused by interface roughness or impurities, which is required for resonant transfer between Landau levels of different subbands. It is clearly seen from the figure that the laser stops working at these magneto-intersubband resonances.

The energy difference between the injector states is small (~3.1 – 3.8 meV [10]) and the condition for complete magnetic quantization

$$\frac{\hbar e B}{m^*} > \Delta E_{injector}$$

is reached at relatively low magnetic fields. Optimum performance of the laser should be achieved for $\frac{\hbar e B}{m^*} M = \Delta E_{injector}$ and $\frac{\hbar e B}{m^*} N \neq \Delta E_{laser}$, where N and M are integers.

The interplay between increased injector efficiency and reduced non-radiative relaxation determines the detailed dependence of the laser intensity on the magnetic field.

The laser intensity increase and oscillatory behavior was consistently observed for all lasing devices independently of device width.

Conclusion

In summary, we have observed a reduction of the threshold current, an enhancement of laser emission intensity and shifts of the emission line in an external magnetic field applied normal to epilayers. An operating range of the selected waveguide design is consistent with our finite-difference time-domain simulation results. The intensity enhancement and the threshold current reduction are attributed to the suppression of nonradiative Auger-intersubband transitions by Landau-quantization of the in-plane electron motion, to the modulation of the injection rate via resonant inter-Landau-level transfer and to the modulation of waveguide properties.

Acknowledgements

We acknowledge support by the Austrian Science Foundation (START, ADLIS SFB) and the European Community IST program (Teravison, Supersmile).

References

[1] R. Köhler, A. Tredicucci, F. Beltram, H.E. Beere, E.H. Linfield, A.G. Davies, D.A. Ritchie, R.C. Iotti, F. Rossi, *Nature* **417**, 156 (2002).

[2] L. Ajili, G. Scalari, D. Hofstetter, M. Beck, J. Faist, H. Beere, G. Davis, E. Linfield, D. Ritchie, *Elect. Lett.* **38**, 1675 (2002).

[3] A. Blank and S. Feng, *J. Appl. Phys.* **74**, 4795 (1993).

[4] J. Ulrich, R. Zobl, K. Unterrainer, G. Strasser, and E. Gornik, *Appl. Phys. Lett.* **76**, 19 (2000).

[5] S. Blaser, M. Rochat, M. Beck, D. Hofstetter and J. Faist, *Appl. Phys. Lett.* **81**, 67 (2002).

[6] K. S. Yee, *IEEE Trans. Antennas Propagat.*, vol. AP-14, pp. 302-307, May 1966.

[7] A. Taflove, *Computational Electrodynamics: The Finite-Difference Time-Domain Method.* Norwood, MA: Artech House, 1995.

[8] R. W. Ziolkowski, J. M. Arnold, D. M. Gogny, *Phys. Rev. A*, vol. 52, 4, pp. 3082-3094, 1995.

[9] M. E. Raikh and T. V. Shahbazyan, *Phys. Rev. B* 49, 5531 (1994).

[10] R. Köhler, R. C. Iotti, A. Tredicucci, F. Rossi, *Appl. Phys. Lett.* **79**, 3920 (2001).

[11] V. Tamosiunas, R. Zobl, J. Ulrich, K. Unterrainer, R. Colombelli, C. Gmachl, K. West, L. Pfeiffer, F. Capasso, *Appl. Phys. Lett.* **83**, 3873 (2003).